An ISB-consistent Denavit-Hartenberg model of the human upper limb for joint kinematics optimization: validation on synthetic and robot data during a typical rehabilitation gesture

An ISB-consistent Denavit-Hartenberg model of the human upper limb for joint kinematics optimization: validation on synthetic and robot data during a typical rehabilitation gesture*

M. Caruso, L. Gastaldi, S. Pastorelli, A. Cereatti and E. Digo

***Abstract*— Several biomedical contexts such as diagnosis, rehabilitation, and ergonomics require an accurate estimate of human upper limbs kinematics. Wearable inertial measurement units (IMUs) represent a suitable solution because of their unobtrusiveness, portability, and low-cost. However, the time-integration of the gyroscope angular velocity leads to an unbounded orientation drift affecting both angular and linear displacements over long observation interval. In this work, a Denavit-Hartenberg model of the upper limb was defined in accordance with the guidelines of the International Society of Biomechanics and exploited to design an optimization kinematics process. This procedure estimated the joint angles by minimizing the difference between the modelled and IMU-driven orientation of upper arm and forearm. In addition, reasonable constraints were added to limit the drift influence on the final joint kinematics accuracy. The validity of the procedure was tested on synthetic and experimental data acquired with a robotic arm over 20 minutes. Average rms errors amounted to 2.8 deg and 1.1 for synthetic and robot data, respectively.**

***Clinical Relevance*— The proposed method has the potential to improve robustness and accuracy of multi-joint kinematics estimation in the general contexts of home-based tele-rehabilitation interventions. In this respect, adoption of multi-segmental kinematic model along with physiological joint constraints could contribute to address current limitations associated to unsupervised analysis in terms of monitoring and outcome assessment.**

I. Introduction

The accurate estimate of the upper limb kinematics is crucial for several biomedical applications such as tele-rehabilitation, clinical evaluation, and ergonomics [1]. Nowadays, wearable inertial measurement units (IMUs) represent a convenient solution to unobtrusively monitor the performance of subjects in ecological environments [2]–[4]. Upper limb angular and linear kinematics can be estimated from multiple IMUs mounted on the upper limb by means of sensor fusion algorithms [5]. However, when computing the orientation of each IMU, the main drawback is the drift caused by the time integration of the angular velocity, which is typically corrupted by a non-stationary bias [6]. The orientation drift of each IMU is then reflected on the joint kinematics estimates, thus resulting in high angular and position errors. To reduce this detrimental effect, it is common to subtract from the gyroscope signal recorded during a dynamic acquisition its mean value computed during a static acquisition. Despite helpful, this procedure is not completely effective. In fact, the bias exhibits non-negligible run-to-run changes due to, for example, temperature changes [6], [7], resulting in a time-variant residuals which cannot be compensated for.

According to the International Society of Biomechanics (ISB), upper limb joint kinematics can be described through five angular degrees of freedom (DoFs) (three at the shoulder and two at the elbow) and one subject-specific parameter, the carrying angle [8]. When the movement does not involve the trunk, a first simple solution to estimate the shoulder angles consists in aligning the upper arm (UA) IMU with the humerus anatomical axes and computing the relative orientation with respect to an initial anatomical posture. The elbow angles can be estimated as the relative orientation between the UA IMU and the IMU attached to the forearm (FA) and aligned with its anatomical axes. A clinically relevant joint kinematics description in terms of Euler angles can be then obtained by decomposing relative orientations according to ISB standard sequences. However, following this approach, errors in the IMUs orientation directly affect the quality of joint kinematics estimates, possibly reflecting in non-physiological joint angular accelerations and ranges of motion. Finally, another limitation of this approach, based on Euler angles decomposition, is the possibility of mathematical singularities. To overcome the above-mentioned issues, we proposed a Denavit-Hartenberg (DH) model to track the upper limb motion consistently with the corresponding ISB convention. The DH notation provides an efficient way for defining a generic robotic chain [9]. The five degrees of freedom of the model (i.e., the joint angles) were obtained at each time step by optimizing the difference between the modelled UA and FA orientation and the one computed with the sensor fusion algorithm combining the accelerometer and gyroscope signals. In addition, this optimization framework allows to set the limit for each joint and to restrict the maximum angular change between two consecutive time steps. The validity of this model was assessed on synthetic and experimental data acquired on a robotic arm reflecting typical rehabilitation exercises [10]. In both cases, to verify the influence of a considerable drift on the final joint angle accuracy, the length of the recordings amounted to about 20 minutes, a typical amount of time for upper limb rehabilitation [10]. Finally, a comparison was made between the joint kinematics estimated within the model-

*Supported by Sardegna Ricerche with POR FESR 2014/2020, Priority Axis I "Scientific Research, Technological Development and Innovation".

M. Caruso and A. Cereatti are with the Departments of Electronics and Telecommunications and Polito^{BIO}Med Lab—Biomedical Engineering Lab, Politecnico di Torino, Torino, Italy (corresponding author phone: +39 3401740484; e-mail: marco.caruso@polito.it).

E. Digo and S. Pastorelli are with Department of Mechanical and Aerospace Engineering, Politecnico di Torino, Torino, Italy (e-mail: elisa.digo@polito.it and stefano.pastorelli@polito.it).

L. Gastaldi is with Department of Mathematical Sciences "G.L. Lagrange" and Polito^{BIO}Med Lab, Politecnico di Torino, Torino, Italy (e-mail: laura.gastaldi@polito.it).

optimization framework and the one computed with the traditional Euler inversion of the relative orientation.

II. Material and Methods

A. DH model of the upper limb

The upper limb was modelled adopting the DH convention in agreement with the guidelines of ISB (Fig. 1). Accordingly, two rigid segments, UA and FA, were identified and a 6-DoFs model was defined. In detail, the shoulder was modelled as a spherical joint with 3 DoFs: the elevation plane (q_1), the elevation (q_2), and the intra-extra rotation (q_3). The elbow was modelled as a universal joint with 2 DoFs: the flexion-extension (q_4) and the pronation-supination (q_6). Moreover, a fixed subject-specific carrying angle (q_5) was introduced to model the physiological abduction of the FA with respect to the UA. Four DH parameters, two distances (d_i and a_i) and two angles (θ_i and α_i), were chosen to identify the pose of the link i with respect to the link i-1. According to the DH convention, three of these parameters (d_i, a_i and α_i) were always constant and depended only on the geometry of connections between consecutive joints. Since all the joints were modelled as revolute ones, the fourth parameter θ_i were the only variable values depending on q_i.

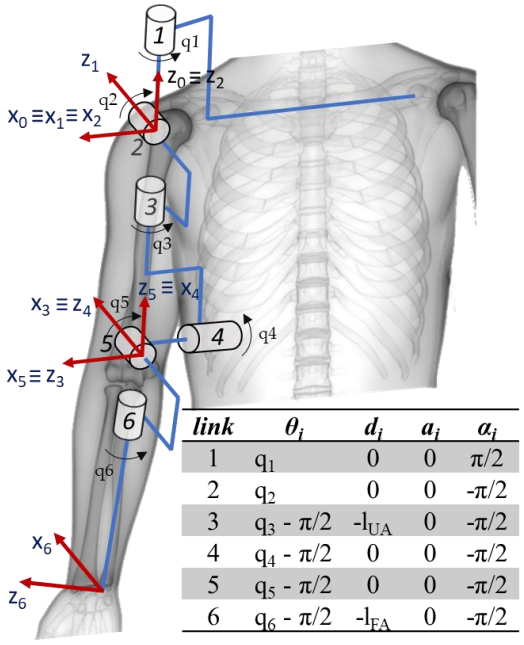

link	θ_i	d_i	a_i	α_i
1	q_1	0	0	π/2
2	q_2	0	0	-π/2
3	q_3 - π/2	$-l_{UA}$	0	-π/2
4	q_4 - π/2	0	0	-π/2
5	q_5 - π/2	0	0	-π/2
6	q_6 - π/2	$-l_{FA}$	0	-π/2

Figure 1. DH model and parameters of the human upper limb.

In the following, the bold notation $\boldsymbol{q}$ refers to the vector [q_1, q_2, q_3, q_4, q_5, q_6]. According to the DH convention [11], it is straightforward to obtain the elbow and wrist orientation matrices, ${}^0_{UA}A$ and ${}^0_{FA}A$, respectively, where axes (x_0, y_0, z_0) of the fixed frame can be assumed coincident with thorax ones.

B. Optimization framework

To estimate the elbow and wrist joint kinematics it is necessary to know the values of $\boldsymbol{q}$. This is accomplished by minimizing, at each time-step, the difference between the orientation estimated using the DH model (${}^0_{UA}R$ and ${}^0_{FA}R$) and the corresponding orientation computed using a sensor fusion algorithm [12] fed with IMU measurements (${}^0_{UA}\hat{R}$ and ${}^0_{FA}\hat{R}$). This process is described in Fig. 2 for each k-th time-step.

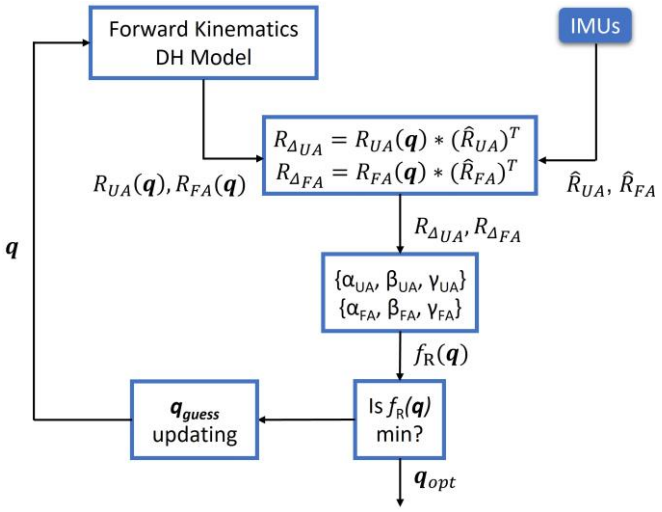

Figure 2. Orientation-based optimization process.

The orientation residuals $R_{\Delta_{UA}}$ and $R_{\Delta_{FA}}$ were then converted in the corresponding angular notation (ZYX sequence) to create the objective function $f_R(\boldsymbol{q})$ which represents the angular difference between the modelled and sensor-fusion based orientations for UA and FA. When the guess $\boldsymbol{q}$ is close to the sensor-fusion based orientation, the $f_R(\boldsymbol{q})$ is small thus not resulting in singularities of the Euler angles. The output of this process is the vector of the optimal DoFs $\boldsymbol{q}_{opt}$ at the current time-step. Each DoF of the optimal solution is bounded between two limits which can be set, by means of Lagrange multipliers, based on both the physiological range of motion of each joint and, if known *a-priori*, the range of the movement under analysis [13]. Furthermore, it is possible to constrain the maximum angular change of each DoF between two consecutive time-steps based on the expected angular velocity. The minimization was performed using a non-linear least squares solver. Initial conditions were set equal to $\boldsymbol{q}_{opt}$ values found at the previous time-step to ease the converge of the solution.

C. Data acquisition

The proposed optimization method was tested using synthetic and robot IMU data. In both cases, data were relative to a single motion involving variation in three DoFs which mimicked a shoulder flexion-extension, an elbow flexion-extension, and a forearm prono-supination, simultaneously.

1) Synthetic data

In this section the process to obtain realistic noisy accelerometer and gyroscope data is described. To simulate the desired motion q_1 and q_3 were set to 90 and -90 deg, while q_2, q_4 and q_6 were varied from 0 to 150 deg and back in 3 s. The trajectory was designed using a 5-th order polynomial and imposing to zero the joint angular velocity and acceleration at 0 and 150 deg [9]. This trajectory was repeated for 400 cycles (~20 minutes, sampling frequency = 100 Hz) to obtain the reference $\boldsymbol{q}_{ref}$. The corresponding ideal IMU signals were generated using the direct kinematics recursive process which evaluates accelerations and angular velocities from DoFs. For each IMU the gravity vector projected on the

local coordinate system was subtracted from the acceleration to obtain the accelerometer output. Then noise was added to the signals of each IMU. Noise characteristics in terms of density, bias instability, and random walk were derived from those computed in static for 18 Xsens – MTw (Xsens, The Netherlands) using the Allan Variance [14]. TABLE I reports the selected values for accelerometers and gyroscopes.

TABLE I. SELECTED NOISE CHARACTERISTICS

Xsens – MTw (18 IMUs)	Accelerometer (mean + 3 STD)		Gyroscope (mean + 3 STD)	
Noise Density	0.0012	$(m/s^2)/\sqrt{Hz}$	0.0079	dps/√Hz
Bias Instability	0.0013	m/s^2	0.0054	dps
Random Walk	6.9181×10^{-5}	$(m/s^2)/\sqrt{Hz}$	0.0004	dps/√Hz

The static noise was generated using the IMU simulation model (Sensor Fusion and Tracking Toolbox, MATLAB R2021b, The MathWorks Inc, MA, USA). To simulate the bias residual of the gyroscope, two static recordings were generated starting from the same seed. Then, the mean value of the first recording was subtracted from the second gyroscope data. Residuals amounted to [0.0233, 0.0270, 0.0184] and [-0.0215 -0.0076 -0.0119] dps for UA and FA data, respectively.

2) Robot data

The collaborative robot chosen for the test was the Kinova Jaco2 (Quebec, Canada) whose maximum angular velocity was 36 dps for all shoulder and elbow actuators, but for prono-supination (48 dps). The robot was firmly fixed on a table. An Ethernet connection was established between the robot and a PC to record data. Acquisitions were made through the software MATLAB at a sampling frequency of about 100 Hz.

The inertial motion capture system was composed of two wireless Xsens-MTw IMUs, both containing a tri-axial accelerometer (range ± 160 m/s^2) and a tri-axial gyroscope (range ± 2000 dps). Before the acquisition, a warm-up period of 10 minutes was executed to limit the influence of the temperature on the gyroscope readings. Then, a static acquisition was performed to compute the gyroscope biases. Then, IMUs were positioned on the arm and forearm of the robot (Fig. 3). Each unit was fixed manually aligning its y-axis with the longitudinal axis of the correspondent robot link. Data were acquired through the Xsens proprietary software MT Manager (v. 4.6) at a sampling frequency of 100 Hz. The robot was positioned in a starting configuration, $\boldsymbol{q}$ = [90 50 -90 0 0 0] and it was programmed to reach the final $\boldsymbol{q}$ = [90 120 -90 150 0 100] at its maximum speed. The robot executed the movement for 20 consecutive minutes (~ 150 cycles).

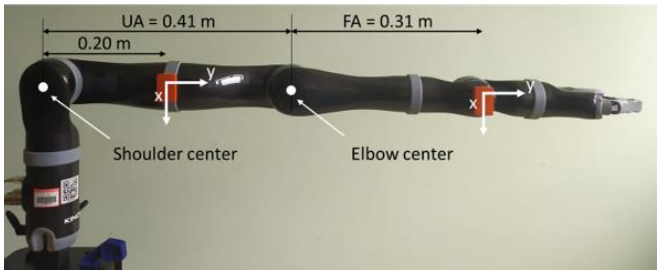

Figure 3. The considered experimental setup.

D. Signal pre-processing and kinematics estimation

1) Synthetic data

The orientation of both UA and FA IMUs was obtained using the sensor fusion filter by Madgwick *et al.*, 2011 [15], separately. Since the parameter value of the filter plays a central role in determining the accuracy of the estimates [12], [16], [17], in this work the orientation was computed using the optimal value for each IMU (i.e., the value which minimized the average orientation error with respect to the reference). The orientation of the two IMUs was obtained in the quaternion form and then converted into rotation matrices.

2) Robot data

The robot data were resampled at 100 Hz using the recorded timestamp to obtain $\boldsymbol{q}_{ref}$ and then synchronized to IMU signals through the cross-correlation [12]. IMU signals were low-pass filtered (8^{th} order Butterworth, cut-off frequency set to 4 Hz) to remove the high-frequency oscillation due to the robot. Then the bias computed in static was removed from the gyroscope readings. To improve the alignment accuracy between IMUs and the robot surface a rotation matrix was computed exploiting the gravity vector. This small rotation was then used to virtually rotate all the measurements. As done for the synthetic signals, the orientation of each unit was obtained using [15] with the corresponding optimal parameter values and then converted into rotation matrix.

In both cases, the orientation matrices obtained with the sensor fusion were used in the optimization process to obtain the $\boldsymbol{q}_{opt}$ vector. Since the motion was planar, q_1 and q_3 were bounded between 90 ± 1 deg, while the others were allowed to span between – 5 and 160 deg (but for the carrying angle q_5 which was set to zero since the robot UA and FA axes are not skewed). Moreover, the maximum angular change between two consecutive time-steps was limited to 2 deg for q_2, q_4, and q_6, and forced to be null for q_5. Finally, to compare the optimization with the traditional methods, the same matrices were used to compute the Euler angles (stored in $\boldsymbol{q}_{Eul}$) using the standard sequence proposed by the ISB convention for the shoulder and the elbow.

E. Error evaluation

For each case, to evaluate the accuracy of the estimates, the following quantities were computed over time $\boldsymbol{e}_{opt}$ = rms($\boldsymbol{q}_{opt} - \boldsymbol{q}_{ref}$) and $\boldsymbol{e}_{Eul}$ = rms($\boldsymbol{q}_{Eul} - \boldsymbol{q}_{ref}$).

III. RESULTS

The $\boldsymbol{e}_{opt}$ and $\boldsymbol{e}_{Eul}$ obtained from synthetic and robot data were reported in TABLE II. In addition, the optimal values for the parameter of the sensor fusion filter amounted to 0.0224 and 0.0005 rad/s for the UA and FA IMUs during simulation and to 0.001 and 0.9 rad/s, respectively when using robot data.

TABLE II. JOINT ANGLE ERRORS

	(deg)	q_1	q_2	q_3	q_4	q_5	q_6
synthetic	$\boldsymbol{e}_{opt}$	0.9	3.7	0.9	3.2	0	7.9
	$\boldsymbol{e}_{Eul}$	13.2	3.8	0.1	3.9	16.1	16.2
robot	$\boldsymbol{e}_{opt}$	1.0	0.4	0.9	3.0	0	1.0
	$\boldsymbol{e}_{Eul}$	10.2	0.2	1.4	3.1	8.2	6.0

IV. Discussion

One of the main critical limitations when estimating the joint kinematics using the low-cost inertial technology over long period consists in the angular drift accumulated as time increases due to the integration of the gyroscope bias residuals. Despite the low values of this residual, the integration over 20 minutes can led to a huge drift, as reported in TABLE II, even if the sensor fusion filter was driven with an optimal parameter value for each IMU in both cases. It is also interesting to observe that different types of motion require to set different optimal parameter values, in line with [12], [16], [17]. When the joint angles were computed with the traditional Euler inversion ($\boldsymbol{e}_{Eul}$), the errors amounted to very large values, especially for the DoFs estimated when IMU axes were aligned along the vertical direction during the motion. During this situation the drift cannot be compensated for by exploiting the gravity direction.

In this work, a DH model of the upper limb was defined to express the joint angle accordingly to the ISB guidelines and to allow the definition of the proper biomechanical constraints. Since the characteristics of motion in terms of speed and range were known *a-priori*, it was possible to introduce these limits in the optimization framework thus leading to lower rms joint angle errors: 2.8 vs 8.9 deg for synthetic data and 1.1 vs 8.9 deg for robot data, respectively, on average. In addition, q_2, q_4, and q_6, errors related to robot data were in general slightly lower when compared to synthetic ones, since the simulation was thought to be more challenging in terms of speed and intensity than the motion characteristics achievable with the robot, due to the technical limitations of the latter. A higher motion intensity resulted in higher acceleration values corrupting the gravity direction estimation. Finally, it must be acknowledged that the proposed optimization framework could not be completely effective in reducing the drift for q_2, q_4, and q_6 as they spanned a large range of motion. However, contrary to the traditional Euler inversion, the proposed method offers the possibility to limit variations between two consecutive time steps within reasonable values, thus mitigating the sensor fusion errors. Current efforts are devoted to exploit the complementary information carried by the linear accelerations and the angular velocities. Indeed, the minimization of multiple objective functions derived from measurements with different source of errors [6] may improve the compensation of the drift.

V. Conclusion

In this work, an optimization framework involving a DH model of the upper limb was proposed to describe its motion consistently with the ISB guidelines using the IMU signals. The obtained joint angular errors suggest exploiting this solution in tele-rehabilitation applications to properly plan the treatment and to accurately evaluate the outcomes.

References

[1] P. Picerno *et al.*, "Upper limb joint kinematics using wearable magnetic and inertial measurement units: an anatomical calibration procedure based on bony landmark identification," *Scientific Reports*, vol. 9, no. 1, pp. 1–10, 2019, doi: 10.1038/s41598-019-50759-z.

[2] C. Mazzà *et al.*, "Technical validation of real-world monitoring of gait: a multicentric observational study," *BMJ Open*, vol. 11, no. 12, p. e050785, Dec. 2021, doi: 10.1136/bmjopen-2021-050785.

[3] E. Digo, G. Pierro, S. Pastorelli, and L. Gastaldi, "Evaluation of spinal posture during gait with inertial measurement units," *Proceedings of the Institution of Mechanical Engineers, Part H: Journal of Engineering in Medicine*, vol. 234, no. 10, pp. 1094–1105, Oct. 2020, doi: 10.1177/0954411920940830.

[4] E. Digo, L. Gastaldi, M. Antonelli, S. Pastorelli, A. Cereatti, and M. Caruso, "Real-time estimation of upper limbs kinematics with IMUs during typical industrial gestures," *Procedia Computer Science*, vol. 200, pp. 1041–1047, Jan. 2022, doi: 10.1016/J.PROCS.2022.01.303.

[5] A. Cereatti, D. Trojaniello, and U. della Croce, "Accurately measuring human movement using magneto-inertial sensors: Techniques and challenges," *2nd IEEE International Symposium on Inertial Sensors and Systems, IEEE ISISS 2015 - Proceedings*, pp. 1–4, 2015, doi: 10.1109/ISISS.2015.7102390.

[6] M. Caruso, A. M. Sabatini, M. Knaflitz, M. Gazzoni, U. della Croce, and A. Cereatti, "Orientation Estimation through Magneto-Inertial Sensor Fusion: A Heuristic Approach for Suboptimal Parameters Tuning," *IEEE Sensors Journal*, vol. 21, no. 3, pp. 3408–3419, 2021, doi: 10.1109/JSEN.2020.3024806.

[7] M. Kirkko-Jaakkola, J. Collin, and J. Takala, "Bias prediction for MEMS gyroscopes," *IEEE Sensors Journal*, vol. 12, no. 6, pp. 2157–2163, 2012, doi: 10.1109/JSEN.2012.2185692.

[8] G. Wu *et al.*, "ISB recommendation on definitions of joint coordinate systems of various joints for the reporting of human joint motion - Part II: Shoulder, elbow, wrist and hand," *Journal of Biomechanics*, vol. 38, no. 5, pp. 981–992, 2005, doi: 10.1016/j.jbiomech.2004.05.042.

[9] B. Siciliano and O. Khatib, *Springer handbook of robotics*, vol. 46, no. 06. Springer, 2009. doi: 10.5860/CHOICE.46-3272.

[10] C. Brogårdh and B. H. Sjölund, "Constraint-induced movement therapy in patients with stroke: A pilot study on effects of small group training and of extended miit use," *Clinical Rehabilitation*, vol. 20, no. 3, pp. 218–227, Mar. 2006, doi: 10.1191/0269215506cr937oa.

[11] V. Cornagliotto, E. Digo, and S. Pastorelli, "Using a Robot Calibration Approach Toward Fitting a Human Arm Model," *Mechanisms and Machine Science*, vol. 102, pp. 199–207, Jun. 2021, doi: 10.1007/978-3-030-75259-0_22.

[12] M. Caruso *et al.*, "Analysis of the Accuracy of Ten Algorithms for Orientation Estimation Using Inertial and Magnetic Sensing under Optimal Conditions: One Size Does Not Fit All," *Sensors*, vol. 21, no. 7, p. 2543, Apr. 2021, doi: 10.3390/s21072543.

[13] M. Begon, M. S. Andersen, and R. Dumas, "Multibody Kinematics Optimization for the Estimation of Upper and Lower Limb Human Joint Kinematics: A Systematized Methodological Review," *Journal of Biomechanical Engineering*, vol. 140, no. 3, pp. 1–11, 2018, doi: 10.1115/1.4038741.

[14] N. El-Sheimy, H. Hou, and X. Niu, "Analysis and modeling of inertial sensors using allan variance," *IEEE Transactions on Instrumentation and Measurement*, vol. 57, no. 1, pp. 140–149, 2008, doi: 10.1109/TIM.2007.908635.

[15] S. O. H. Madgwick, A. J. L. Harrison, and R. Vaidyanathan, "Estimation of IMU and MARG orientation using a gradient descent algorithm," *IEEE International Conference on Rehabilitation Robotics*, p. 2020, 2011, doi: 10.1109/ICORR.2011.5975346.

[16] M. Caruso, A. M. Sabatini, M. Knaflitz, U. della Croce, and A. Cereatti, "Extension of the Rigid-Constraint Method for the Heuristic Suboptimal Parameter Tuning to Ten Sensor Fusion Algorithms Using Inertial and Magnetic Sensing," *Sensors*, vol. 21, no. 18, p. 6307, Sep. 2021, doi: 10.3390/s21186307.

[17] D. Laidig, M. Caruso, A. Cereatti, and T. Seel, "BROAD—A Benchmark for Robust Inertial Orientation Estimation," *Data (Basel)*, vol. 6, no. 7, 2021, doi: 10.3390/data6070072.